The influence of different support movements and heights of piers on the dynamic behavior of bridges. Part I: Earthquake acting transversely to the deck

George T. Michaltsos[†] and Ioannis G. Raftoyiannis[‡]

*Laboratory of Steel Structures, Department of Civil Engineering, National Technical University of Athens,
9 Iroon Polytechneiou St., Zografou Campus, Athens 15780, Greece*

Abstract. This paper presents a simple model for studying the dynamic response of multi-span bridges resting on piers with different heights and subjected to earthquake forces acting transversely to the bridge, but varying spatially along its length. The analysis is carried out using the modal superposition technique, while the solution of the resulting integral-differential equations is obtained via the Laplace transformation. It has been found that the piers' height and the quality of the foundation soil can affect significantly the dynamic behavior of such bridges. Typical examples showing the effectiveness of the method are presented with useful results listed.

Keywords: bridge dynamics; piers; earthquake actions; transverse motion.

1. Introduction

Spatial variability of strong earthquake motions over small distances is a problem frequently encountered in engineering. This variation though, in the temporal and frequency characteristics of the ground motion, produces in long structures forces, which are absent in structures subjected to uniform excitation.

The most important factors causing this spatial variability include the following: (a) non-homogeneity of the ground material, (b) the nature of the seismic excitation propagating waves, which lead to different arrival times at the supports, (c) drop of the wave amplitude in small distances due to geometric and material energy dissipation possibly caused by existing faults, and (d) variable ground conditions leading to different surface motions along the structure.

With reference to bridges, the effect of non-uniform seismic excitation on the structural response has been studied extensively for more than four decades. One must refer to the works of Bogdanoff *et al.* (1965), who first studied the problem for long structures, Harichandran and Wang (1990), who studied the response of a two-span beam under spatially varying seismic excitation, Zerva (1990), who studied the response of multi-span beams, Abrahamson *et al.* (1991), who presented empirical functions for the spatial coherency, Betti *et al.* (1993), who studied the soil-structure interaction on

---

† Professor, Corresponding author, E-mail: michalts@central.ntua.gr
‡ Assistant Professor, E-mail: rafto@central.ntua.gr

long-span cable-stayed bridges, Monti *et al.* (1996), who studied the response of bridges under non-synchronous supports excitations, Price and Eberhard (1998), who studied the effect of spatially varying ground motions on short bridges, and Nikolaou *et al.* (2001), who studied the same problem by kinematical methods.

Eurocode 8-Part 2 (EC8-2 2002) provides detailed instructions for the piers' non-synchronous movements and the spatial variability of earthquakes motions. For piers with different heights, it suggests consideration of the influence of the height on the dynamic behavior of the bridge deck. In particular, EC8-2 refers to this problem in §2.4 and suggests to design such bridges with a continuous deck, if using short pylons is not possible, for their better dynamical behavior than the ones with hinged joints (§2.4.4). Moreover, EC8-2 suggests the use of a very unfavorable distribution of the transverse seismic action (§2.4.6). No further comments or instructions are provided in EC8.

In this work, a simple analytical model is developed for studying the response of a long bridge on either tall or short piers subjected to a spatially varying ground motion. Neglecting the shear deformation, the proposed model can be analyzed as a bridge-deck continuous beam (with known eigenshapes V_n and eigenfrequencies ω_n) and the pylon as a cantilever beam (with also known eigenshapes $\overline{V}_n$ and eigenfrequencies $\overline{\omega}_n$).

Employing the "influence functions" $g(x)$ for the bridge-deck and $\overline{g}(\overline{x})$ for each pier (which express the deformed configuration of a beam with unit displacement at each support), and using the modal analysis technique, along with the compatibility condition at the supports, one can finally arrive at the integral-differential equations in terms of the time functions for the joint motions. The above equations are solved through the Laplace transformation and the relations obtained are evaluated numerically by the Mathematica symbolic manipulator. Typical examples showing the effectiveness of the method are presented with useful results tabulated.

The proposed method utilizes the characteristic of the transverse eigenshapes nullification at the supports and thus, it cannot be applied for the case of motion acting in a direction parallel to the deck. This case is solved in a completely different manner, which is the subject of a companion publication.

Finally, it should be noted that in the present work an analytical model for studying the dynamical behavior of bridges on tall and unequal piers is proposed, which has no relation to the wave propagation in soil. Therefore, the examples studied will be used as a vehicle to illustrate the effects considered.

2. Basic assumptions

The bridge shown in Fig. 1 is resting on a number of piers fixed (or pinned) on the ground. In this study, and without loss of generality, we consider piers fixed at their bases, but with joints at the bottom side of the deck free to rotate (see Figs. 1 and 2). We also assume that each pier is subjected to different base motion, and hence, the base displacement of the ith pier is denoted with $f_i(t)$. The axial and shear deformations for both the bridge-deck and the piers are neglected.

We assume that the top of the ith pier is moving according to the time function $\varphi_i(t)$ that is to be determined. All data concerning the piers will be over lined within the text. The above system can be analyzed as a bridge-deck continuous beam (Fig. 2a), for which the shape functions V_ns and the
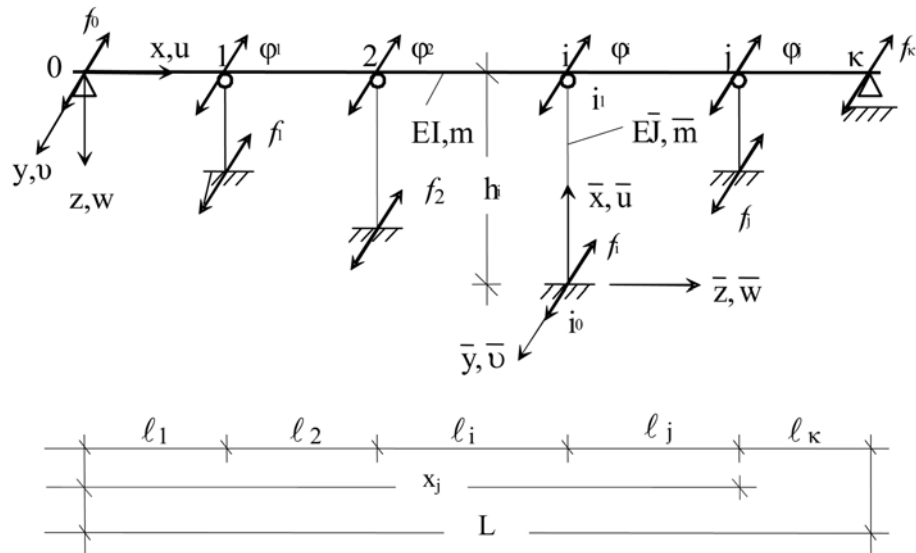
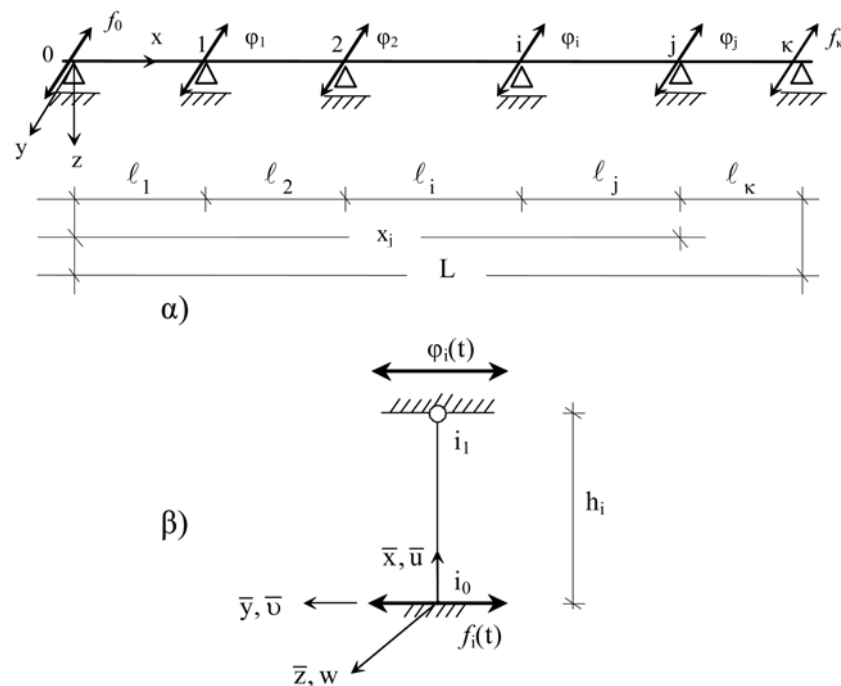Fig. 1 A typical bridge on piers with different movements

Fig. 2 Model of the bridge-deck and pylon beam system

eigenfrequencies ω_n are known, and as single-pylon beams (Fig. 2b) with also known shape functions $\overline{V}_{in}$ and eigenfrequencies $\overline{\omega}_{in}$.

The "influence functions" $g_i(x)$ for the bridge-deck and $\bar{g}_i(\bar{x})$ for each pier are also known since we consider a unit displacement at the supports i. The time functions f_i at the supports are known, while the time functions φ_i at the joints are to be determined.

3. Analytical model

The total displacement of the bridge-deck beam along the y-axis is given by

$$\upsilon(x,t) = \upsilon_o(x,t) + \upsilon_{st}(x,t) = \upsilon_o(x,t) + \sum_{j=1}^{\kappa-1} g_j(x)\varphi_j(t) + g_o(x)f_o(t) + g_\kappa(x)f_\kappa(t) \tag{1}$$

where υ_o is the "elastic deformation", υ_{st} is the "static or geometric deformation" due to the supports displacements, φ_j are the time functions, g_o, g_κ are the influence functions corresponding to the left and right support, respectively, and g_j are the influence functions corresponding to the intermediate supports. The equation of motion of the beam is: $EI_z \upsilon'''' + c\dot{\upsilon} + m\ddot{\upsilon} = 0$. Introducing υ from Eq. (1) into this equation, we obtain

$$EI_z \upsilon_o'''' + c\dot{\upsilon}_o + m\ddot{\upsilon}_o = -m\sum_{j=1}^{\kappa-1} g_j(x)\ddot{\varphi}_j(t) - mg_o(x)\ddot{f}_o(t) - mg_\kappa(x)\ddot{f}_\kappa(t) \tag{2}$$

We search for a solution of the form

$$\upsilon_o(x,t) = \sum_n V_n(x)T_n(t) \tag{3}$$

where $V_n(x)$ are the shape functions of the bridge-deck system (continuous beam) and $T_n(t)$ is the time function to be determined. Introducing υ_o from Eq. (3) into Eq. (2), we obtain

$$EI_z \sum_n V_n'''' T_n + c\sum_n V_n \dot{T}_n + m\sum_n V_n \ddot{T}_n = -m\sum_{j=1}^{\kappa-1} g_j(x)\ddot{\varphi}_j(t) - mg_o(x)\ddot{f}_o(t) - mg_\kappa(x)\ddot{f}_\kappa(t) \tag{4}$$

Since the shape functions $V_n(x)$ satisfy the equation of free motion: $EI_z V_n'''' - m\omega_n^2 V_n = 0$, Eq. (4) will take the following form

$$\sum_n V_n \ddot{T}_n + \frac{c}{m}\sum_n V_n \dot{T}_n + \sum_n \omega_n^2 V_n T_n = -\sum_{j=1}^{\kappa-1}\left(\ddot{\varphi}_j \sum_n A_{jn} V_n\right) - \sum_n A_{on} V_n \ddot{f}_o - \sum_n A_{\kappa n} V_n \ddot{f}_\kappa \tag{5a}$$

where

$$A_{jn} = \frac{\int_0^L g_i(x)V_n(x)dx}{\int_0^L V_n^2(x)dx}, \quad A_{on} = \frac{\int_0^L g_o(x)V_n(x)dx}{\int_0^L V_n^2(x)dx}, \quad A_{\kappa n} = \frac{\int_0^L g_\kappa(x)V_n(x)dx}{\int_0^L V_n^2(x)dx} \tag{5b}$$

and the functions g_i, g_o, g_κ have been expressed in terms of the eigenshapes $V_n(x)$. Multiplying Eq. (5a) by V_n, integrating from 0 to L (length of the entire bridge), and taking into account the orthogonality condition, one can obtain

$$\ddot{T}_n + \frac{c}{m}\dot{T}_n + \omega_n^2 T_n = -\sum_{j=1}^{\kappa-1} A_{jn} H\left(t - \sum_{\rho=1}^{j}\frac{l_\rho}{v}\right)\ddot{\varphi}_j(t) - A_{on}\ddot{f}_o(t) - A_{\kappa n}H\left(t - \frac{L}{v}\right)\ddot{f}_\kappa(t) \tag{6}$$

where v is the wave's propagation velocity of the soil, H(x-a) is the Heaviside's unit step function, l_ρ is the length of the length of the ρth span, and ω_n is the nth eigenfrequency. Eq. (6), with initial conditions $T_n(0) = \dot{T}_n(0) = 0$, has the following solution given by the Duhamel's second integral

$$T_n(t) = -\sum_{j=1}^{\kappa-1}\left(\frac{A_{jn}}{\tilde{\omega}_n}\int_0^t H\left(\tau - \sum_{\rho=1}^{j}\frac{l_j}{v}\right)e^{-\beta(t-\tau)}\ddot{\varphi}_j(\tau)\cdot\sin\tilde{\omega}_n(t-\tau)d\tau\right)$$

$$-\int_0^t\frac{A_{on}}{\tilde{\omega}_n}e^{-\beta(t-\tau)}\ddot{f}_o(\tau)\sin\tilde{\omega}_n(t-\tau)d\tau - \int_0^t\frac{A_{on}}{\tilde{\omega}_n}H\left(\tau-\frac{L}{v}\right)e^{-\beta(t-\tau)}\ddot{f}_o(\tau)\sin\tilde{\omega}_n(t-\tau)d\tau \tag{7a}$$

where

$$\beta = \frac{c}{2m}, \quad \tilde{\omega}_n^2 = \omega_n^2 - \beta^2 \tag{7b}$$

The total displacement of the jth fixed-joined pier along the $\bar{y}$ axis is

$$\bar{v}_j(\bar{x}, t) = \bar{v}_{jo}(\bar{x}, t) + \bar{v}_{jst}(\bar{x}, t) = \bar{v}_{jo}(\bar{x}, t) + \bar{g}_{jo}(\bar{x})f_j(t) + \bar{g}_{jl}(\bar{x})\varphi_j(t) \tag{8}$$

where v_o is the elastic deformation, v_{st} is the static one due to the displacement $f_j(t)$ of the foundation and $\varphi_j(t)$ is the displacement at top of the pier.

The equation of motion for the jth pier is: $E\bar{I}_{jz}\bar{v}_j'''' + \dot{\overline{c v}}_j + \bar{m}_j\ddot{\bar{v}}_j = 0$. Introducing $\bar{v}_j$ from Eq. (8) into this expression, we obtain

$$E\bar{I}_{jz}\bar{v}_j'''' + \dot{\overline{c v}}_o + \bar{m}_j\ddot{\bar{v}}_{jo} = -\bar{m}_j\bar{g}_{jo}(\bar{x})\ddot{f}_j(t) - \bar{m}_j\bar{g}_{jl}(\bar{x})\ddot{\varphi}_j(t) \tag{9}$$

We are searching for a solution in the form

$$\bar{v}_{jo}(\bar{x}, t) = \sum_n \bar{V}_{jn}(\bar{x})P_n(t) \tag{10}$$

where $\bar{V}_{jn}(\bar{x})$ are the shape functions of the jth pier and $P_n(t)$ are the corresponding time functions. Thus, Eq. (8) becomes

$$\bar{v}_j(\bar{x}, t) = \sum_n \bar{V}_{jn}(\bar{x})P(t) + \bar{g}_{jo}(\bar{x})f_j(t) + \bar{g}_{jl}(\bar{x})\varphi(t) \tag{11}$$

The two displacements at the j-node must be equal and hence, the following equation is valid: $v(x_j, t) = \bar{v}(h_j, t)$, or because of Eqs. (1), (3) and (11), this equation of compatibility can be written as

$$\sum_n V_n(x_j)T_n(t) + g_o(x_j)f_o(t) + \sum_{i}^{\kappa-1} g_i(x_j)\varphi_i(t) + g_\kappa(x_j)f_\kappa(t) =$$
$$= \sum_n \bar{V}_{jn}(h_j)P_n(t) + \bar{g}_{jo}(h_j)f_j(t) + \bar{g}_{jl}(h_j)\varphi_j(t) \tag{12}$$

At the joint j, where $x = x_j$, the following equations are valid

$$V_n(x_j) = 0$$

$$g_i(x_j) = \begin{cases} 0 \text{ for } i \neq j \\ 1 \text{ for } i = j \end{cases}$$

$$g_{jl}(h_j) = 1, g_{jo}(h_j) = 0 \tag{13}$$

Thus, Eq. (12) becomes: $\varphi_j(t) = \sum_n \overline{V}_{jn}(h_j)P_n(t) + \varphi_j(t)$, or

$$\sum_n \overline{V}_{jn}(h_j)P_n(t) = 0 \tag{14}$$

where $P_n(t)$ is the time function to be determined.

Introducing $\overline{v}_{jo}$ from Eq. (10) into Eq. (9), and following a similar process like the one for the solution of Eq. (4), we arrive at the following relations

$$\ddot{P}_n + \frac{\overline{c}}{\overline{m}_j}\dot{P}_n + \overline{\omega}_{jn}^2 P_n = -\overline{A}_{jon}\ddot{f}_j(t) - \overline{A}_{jln}\ddot{\varphi}_j \tag{15a}$$

where

$$\overline{A}_{jon} = \frac{\int_0^{hi}\overline{g}_{jo}(\bar{x})\overline{V}_{jn}(\bar{x})dx}{\int_0^{hi}\overline{V}_{jn}^2(\bar{x})dx}, \overline{A}_{jln} = \frac{\int_0^{hi}\overline{g}_{jl}(\bar{x})\overline{V}_{jn}(\bar{x})dx}{\int_0^{hi}\overline{V}_{jn}^2(\bar{x})dx} \tag{15b}$$

Eq. (15), with initial conditions: $P_n(0) = \dot{P}_n(0) = 0$, has the following solution, as given by Duhamel's integral

$$P_n(t) = -\frac{\overline{A}_{jon}}{\overset{*}{\omega}_{jn}}\int_0^t e^{-\overline{\beta}(t-\tau)}\ddot{f}_j(\tau)\sin\overset{*}{\omega}_{jn}(t-\tau)d\tau - \frac{\overline{A}_{jln}}{\overset{*}{\omega}_{jn}}\int_0^t e^{-\overline{\beta}(t-\tau)}\ddot{\varphi}_j(\tau)\sin\overset{*}{\omega}_{jn}(t-\tau)d\tau \tag{16a}$$

where

$$\overline{\beta} = \frac{\overline{c}}{2m}, \overset{*}{\omega}_{jn} = \sqrt{\overline{\omega}_{jn}^2 - \overline{\beta}^2} \tag{16b}$$

Introducing P_n from Eq. (16) into Eq. (14), we get the following equation in expanded form

$$\sum_n\left\{\overline{V}_{jn}(h_j)\cdot\frac{\overline{A}_{jln}}{\overset{*}{\omega}_{jn}}\int_0^t e^{-\overline{\beta}(t-\tau)}\ddot{\varphi}_j(\tau)\sin\overset{*}{\omega}_{jn}(t-\tau)d\tau\right\} =$$

$$= -\sum_n\left\{\overline{V}_{jn}(h_j)\cdot\frac{\overline{A}_{jon}}{\overset{*}{\omega}_{jn}}\int_0^t e^{-\overline{\beta}(t-\tau)}\ddot{f}_j(\tau)\sin\overset{*}{\omega}_{jn}(t-\tau)d\tau\right\} \tag{17}$$

which is valid for $j = 1$ to κ-1. From the above (κ-1) Eq. (17) and using Laplace's transformation we can determine the (κ-1) unknowns φ_1, φ_2, ..., $\varphi_{1\,\kappa-1}$, as described below. First, we set

$$L\,\varphi_j(t) \;=\; \Phi_j(p)$$

$$L\,\ddot{\varphi}_j(t) \;=\; p^2\Phi_j(p) - p\,\varphi_j(0) - \dot{\varphi}_j(0) \;=\; p^2\Phi_j(p)$$

$$L(e^{-\beta t}\sin\omega t) \;=\; \frac{\omega}{(p+\beta)^2 + \omega^2}$$

$$Lf(t) \;=\; F(p) \tag{18}$$

with the initial conditions: $\varphi(0) \;=\; \dot{\varphi}(0) \;=\; 0$. By Laplace's transformation and Borel's theorem (Wylie 1975), one can derive from Eq. (17) the following

$$\Phi_j(p)\cdot\sum_n \overline{V}_{jn}(h_j)\overline{A}_{j\,ln}\cdot\frac{\overset{*}{\omega}_{jn}^{\,2}}{(p+\overline{\beta})^2 + \overset{*}{\omega}_{jn}^{\,2}} \;=\; -F_j(p)\cdot\sum_n \overline{V}_{jn}(h_j)\overline{A}_{jon}\cdot\frac{\overset{*}{\omega}_{jn}^{\,2}}{(p+\overline{\beta})^2 + \overset{*}{\omega}_{jn}^{\,2}} \tag{19}$$

which can also be written in the following form

$$\Phi_j(p) \;=\; -F_j(p)\frac{\displaystyle\sum_n \overline{V}_{jn}(h_j)\overline{A}_{jon}\frac{\overset{*}{\omega}_{jn}^{\,2}}{(p+\overline{\beta})^2 + \overset{*}{\omega}_{jn}^{\,2}}}{\displaystyle\sum_n \overline{V}_{jn}(h_j)\overline{A}_{j\,ln}\frac{\overset{*}{\omega}_{jn}^{\,2}}{(p+\overline{\beta})^2 + \overset{*}{\omega}_{jn}^{\,2}}} \tag{20}$$

Solution of the above linear system gives the unknowns $\Phi_j(p)$ under the form

$$\Phi_j(p) \;=\; \frac{N_j(p)}{Q_j(p)} \tag{21}$$

where $N_j(p)$ and $Q_j(p)$ are polynomials with respect to p, and the terms Q_j are of order higher than the terms N_j. Thus, Heaviside's rule can be applied to yield the following expression for the time function $\varphi_j(t)$

$$\varphi_j(t) \;=\; L^{-1}\Phi_j(p) \;=\; L^{-1}\!\left(\frac{N_j(p)}{Q_j(p)}\right) \;=\; \sum_{r=1}^{\sigma} \frac{N_r(p_r)e^{p_r t}}{Q_r(p_r)} \tag{22}$$

where p_r are the roots of the polynomial Q_r. Introducing the expressions for $\varphi_j(t)$ into Eqs. (7) and (15), we can determine the time functions $T_n(t)$ and $P_n(t)$, accordingly.

4. Numerical results and discussion

In this section, we shall apply the above relations to three typical cases. The first one refers to a single-span bridge with non-synchronous support movements. The second one refers to a two-span bridge whose middle support lies on piers of the cantilever type with heights h_1, while all supports are assumed to move in the same way. In this second case, we shall study the influence of the pier's height on the dynamic behavior of the bridge. Finally, in the third case, a three-span bridge will be studied with non-synchronous support movements.

Some assumptions are adopted for the support movements. The movements of supports 0 and j of the bridge are assumed to vary according to the following expressions

$$f_o = a \cdot e^{-bt} \sin \omega_e t$$

$$\text{and} \quad f_j = k_j \cdot a \cdot e^{-bt} \sin(\omega_e t - \rho_j) \tag{23}$$

where ω_e is the cyclic frequency of the harmonic seismic waves. For the cases studied, $a = 0.05$, is the maximum amplitude of the ground motion at the first pier, f_j is the movement at the j^{st} pier, and

$$k_j = -\cos \rho_j + \sqrt{5 \cdot \cos^2 \rho_j - 1} \tag{24}$$

is a coefficient showing the decrease of ground movement as the distance from the epicenter increases, $b = 0.2$ is a constant expressing the damping of the earthquake, the cyclic frequency of the seismic waves ω_e taking values from 1 to 15 for the cases studied, and ρ_j is the phase angle due to the distance L_j between the two supports 0 and j, given by the relation (Zerva 1999)

$$\rho_j = \omega_e \cdot L_j / v \tag{25}$$

where v is the wave propagation velocity of the ground. The value v depends on the ground and is taken as 5.5 km/sec for granite soil and 1.5 km/sec for mud soil.

Since the purpose of this paper is to study the effects of different movements and heights of piers on the dynamic behavior of bridges, but not on the contents of these movements, the above simple expressions given by Zerva (1990, 1999), instead of the more complicated ones of EC 8, will be adopted. Two values will be considered for ω_e: $\omega_e = 3 \text{ sec}^{-1}$, which corresponds to an earthquake of distant source, and $\omega_e = 15 \text{ sec}^{-1}$, which corresponds to an earthquake of near source.

4.1. The single-span bridge

We consider a single-span bridge, made of isotropic and homogeneous material with modulus of elasticity $E = 2.1*10^8 \text{ KN/m}^2$, length $L = 60$ m, mass per unit length $m = 1000$ kg/m, and transverse moment of inertia $I_z = 10 \text{ m}^4$. The data listed in Table 1 are adopted.

Figs. 3 and 4 show the influence of different ground properties on the seismic excitations of the first and second supports. The first three transverse eigenfrequencies of the bridge can be computed as: $\omega_1 = 39.729$, $\omega_2 = 158.916$, and $\omega_3 = 357.560 \text{ sec}^{-1}$. For the influence functions given in the

Table 1 Values of the phase angle ρ and the coefficient k for various soil types

Cyclic frequency	$v = 5500$ m/sec (granite soil)		$v = 2500$ m/sec (mid-quality soil)		$v = 1500$ m/sec (mud soil)	
	ρ	k	ρ	k	ρ	k
$\omega_e = 3$	0.033	0.9992	0.072	0.9961	0.12	0.9892
$\omega_e = 15$	0.164	0.9798	0.36	0.9024	0.60	0.7257
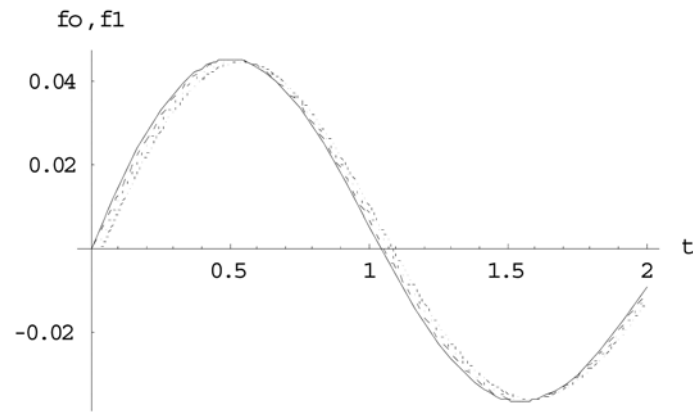
Fig. 3 Seismic excitations of the first support (continuous line) and second support for $\omega = 3$ sec^{-1}, $\rho = 0.033$, $k = 0.9992$ (- - -) (granite), $\rho = 0.072$, $k = 0.9961$ (- - -) (middle), $\rho = 0.12$, $k = 0.9892$ (....) (mud)
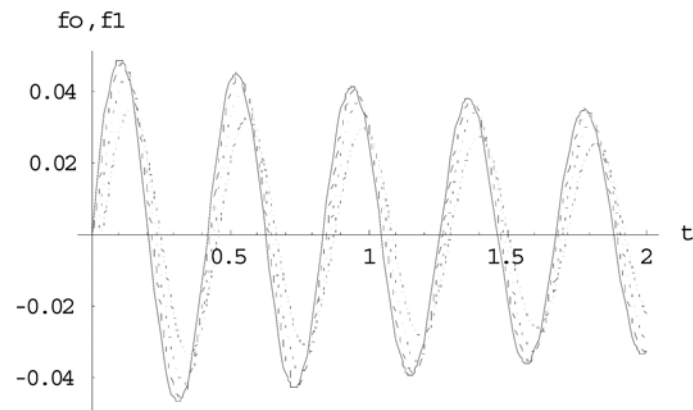
Fig. 4 Seismic excitations of the first support (continuous line) and second support for $\omega = 15$ sec^{-1}, $\rho = 0.164$, $k = 0.9798$ (- - -) (granite), $\rho = 0.36$, $k = 0.9024$ (- - -) (middle), $\rho = 0.60$, $k = 0.7257$ (....) (mud)

Appendix, we find from Eq. (5b)

$$A_{on} = \frac{2}{n\pi} \quad , \quad A_{ln} = \frac{2\cos n\pi}{n\pi}$$

For $\varphi_j(t) = 0$, one can obtain from Eq. (7) the time function $T_n(t)$ as

$$T_n(t) = -\int_0^t \frac{A_{on}}{\tilde{\omega}_n} e^{-\beta(t-\tau)} \ddot{f}_o(\tau) \sin \tilde{\omega}_n(t-\tau) d\tau - H\left(t-\frac{L}{v}\right) \int_0^t \frac{A_{on}}{\tilde{\omega}_n} e^{-\beta(t-\tau)} \ddot{f}_o\left(\tau-\frac{L}{v}\right) \sin \tilde{\omega}_n(t-\tau) d\tau \quad (26)$$

and the displacement $\upsilon(x, t)$ as

$$\upsilon(x, t) = \sum_n V_n(x) T_n(t) + g_o(x) f_o(t) + H\left(t-\frac{L}{v}\right) g_l(x) f_l(t) \quad (27)$$

We will study now the variation of the displacement υ at the mid-span of the bridge for each one of the above soil properties with the aid of Figs. 5 to 10.
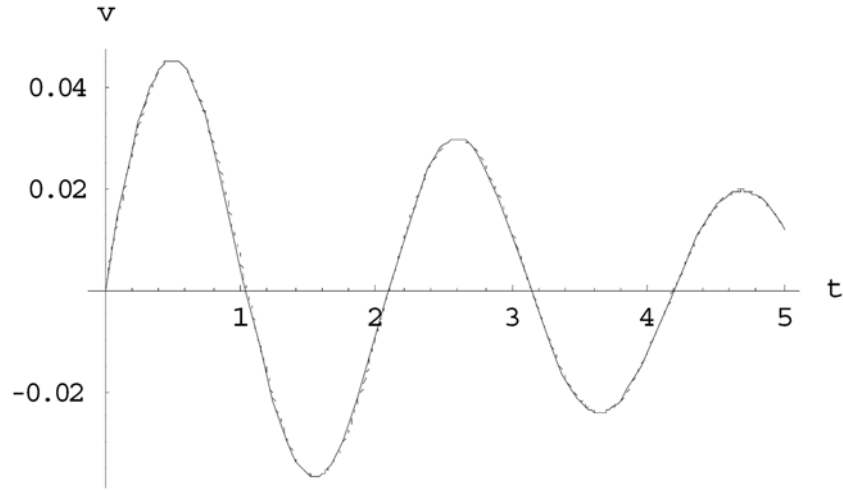
Fig. 5 Displacement of the mid-span of the bridge for $\omega_e = 3$ sec^{-1} and granite soil (continuous line = synchronous support motion, dashed line = non-synchronous support motion)
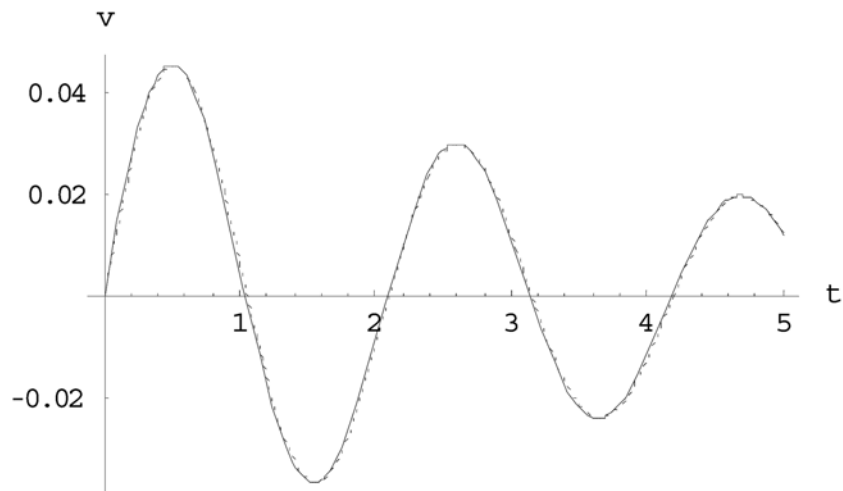
Fig. 6 Displacement of the mid-span of the bridge for $\omega_e = 3$ sec^{-1} and middle soil (continuous line = synchronous support motion, dashed line = non-synchronous support motion)
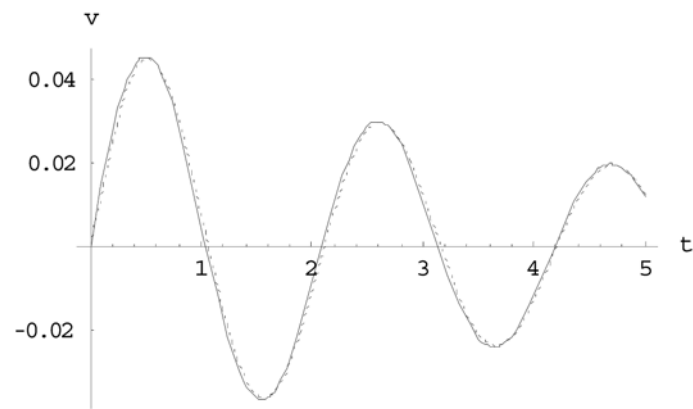
Fig. 7 Displacement of the mid-span of the bridge for $\omega_e = 3$ sec^{-1} and mud soil (continuous line = synchronous support motion, dashed line = non-synchronous support motion)
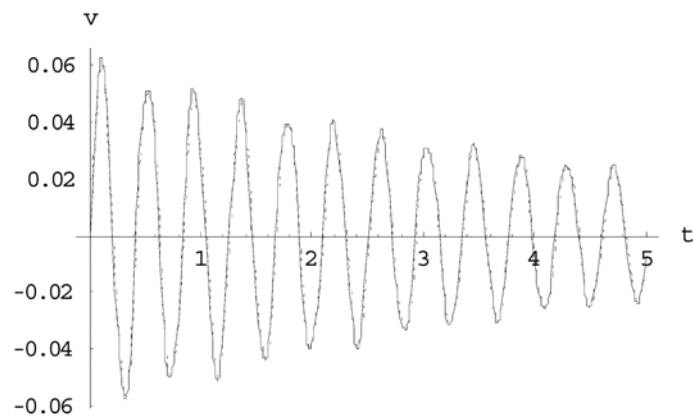
Fig. 8 Displacement of the mid-span of the bridge for $\omega_e = 15$ sec^{-1} and granite soil (continuous line = synchronous support motion, dashed line = non-synchronous support motion)
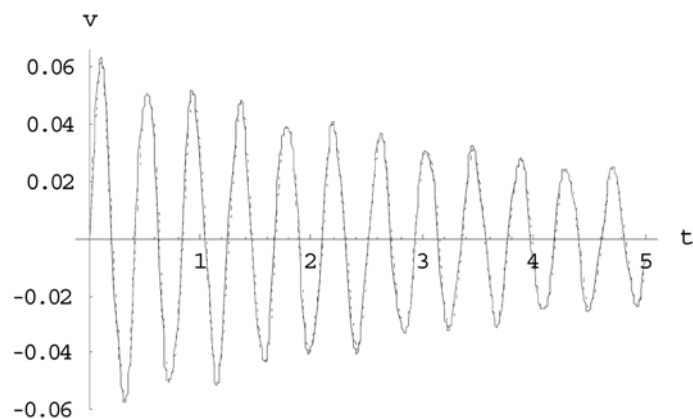
Fig. 9 Displacement of the mid-span of the bridge for $\omega_e = 15$ sec^{-1} and middle soil (continuous line = synchronous support motion, dashed line = non-synchronous support motion)
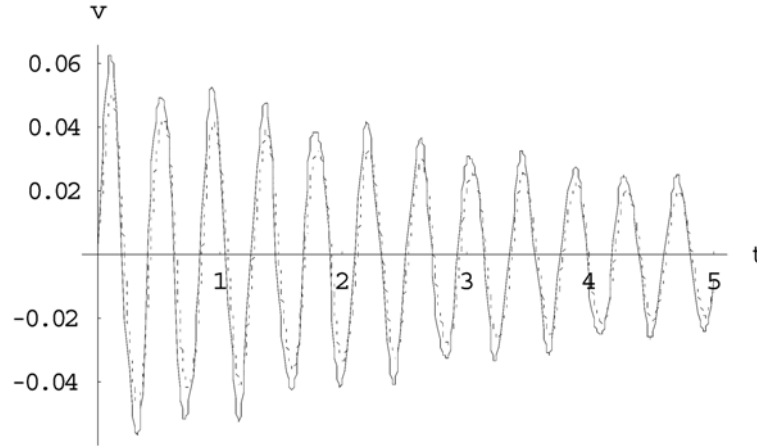
Fig. 10 Displacement of the mid-span of the bridge for $\omega_e = 15$ sec^{-1} and mud soil (continuous line = synchronous support motion, dashed line = non-synchronous support motion)

From the above figures, one observes that the maximum amplitude occurs during the first cycles of oscillation of the bridge. Even for supports spanned at short distances, like the one of the present example ($L = 60$ m), one must take into account the variation in the earthquake's intensity, especially for non-cohesive soils under the action of high frequency motions. The differences in the deck's deformations may range from 0% to 3% for a granite soil, and from 3.5% to 28% for a mud one, where the lower limits correspond to low frequency motions and the higher limits correspond to high frequency motions.

4.2 Effect of the piers' height (two-span bridge)

We consider next a two-span bridge with a deck that has the same properties as those of the example in Section 4.1, and spans of lengths $L_1 = 60$ m, and $L_2 = 70$ m, with its middle support lying on the top of a pylon of height h_1. In addition, we assume that the movements of the ground along the whole length of the bridge are governed by the same equation of ground motion: $f_0 = f_1 = f_2 = a \cdot e^{-bt} \sin \omega_e t$, where a, b, ω_e were given in Section 4.1.

The eigenfrequencies of the two-span beam can be computed as: $\omega_1 = 32.761$, $\omega_2 = 55.210$, and

$\omega_3 = 127.869$ sec^{-1}, and those of the cantilever as: $\overline{\omega}_n = \sqrt{\dfrac{\lambda_n^4 E I_{pylon}}{m_{pylon}}}$, with $\lambda_1 = 1.875/h_1$, $\lambda_2 = 1.5\ \pi/h_1$,

$\lambda_3 = 2.5\ \pi/h_1$ where, $m_{pylon} = 1000$ kg/m and for $I_{pylon} = 0.20$ m^4, 0.80 m^4, and 2.00 m^4. Using the influence functions and shape functions and applying the procedure described in Section 3, one can solve the integral differential system to obtain the time functions φ_j (t), and along with the aid of Eq. (1), study the influence of the pier height h_1 on the bridge displacement w (x, t). Figs. 11, 12, and 13 show the oscillation of the middle support (as indicated by the functions φ_1 (t)) for the pier heights $h = 10, 30, 50$, and 70 m, along with the values of I_{pylon} given above.

Figs. 14, 15, and 16 show the displacement of the deck, at the instant t, when the functions φ_1 take their maximum value.
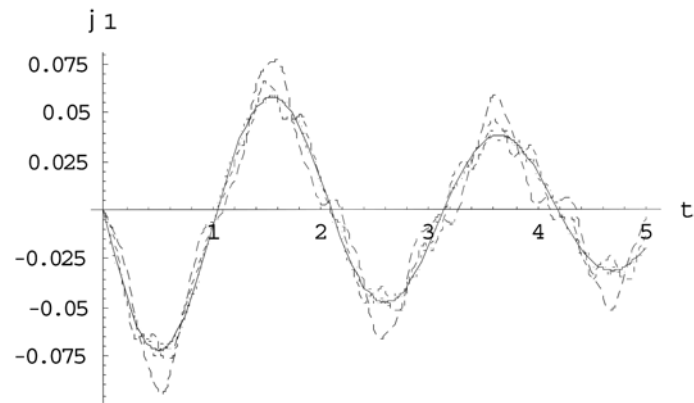
Fig. 11 Time function φ_1 for $I_{pylon} = 0.2\ \mathrm{m}^4$, and for pier heights $h_1 = 10\ \mathrm{m}$(____), $h_1 = 30\ \mathrm{m}$(....), $h_1 = 50\ \mathrm{m}$ (_ _ _), $h_1 = 70\ \mathrm{m}$ (__ __)
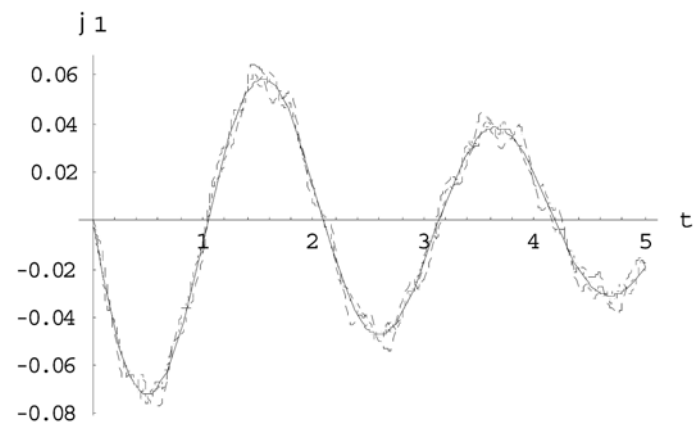
Fig. 12 Time function φ_1 for $I_{pylon} = 0.8\ \mathrm{m}^4$, and for pier heights $h_1 = 10\ \mathrm{m}$(____), $h_1 = 30\ \mathrm{m}$(....), $h_1 = 50\ \mathrm{m}$ (_ _ _), $h_1 = 70\ \mathrm{m}$ (__ __)
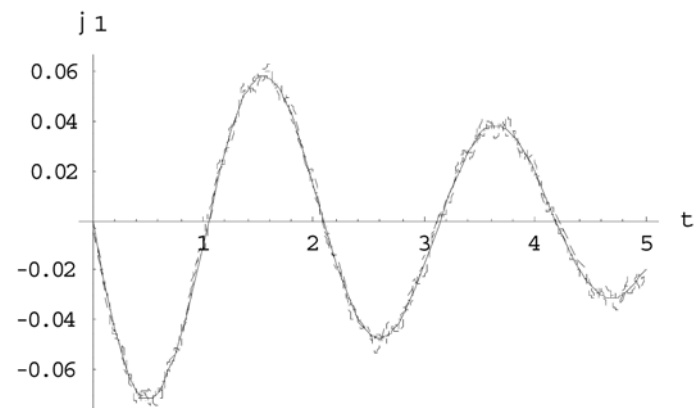
Fig. 13 Time function φ_1 for $I_{pylon} = 2\ \mathrm{m}^4$, and for pier heights $h_1 = 10\ \mathrm{m}$(____), $h_1 = 30\ \mathrm{m}$(....), $h_1 = 50\ \mathrm{m}$ (_ _ _), $h_1 = 70\ \mathrm{m}$ (__ __)
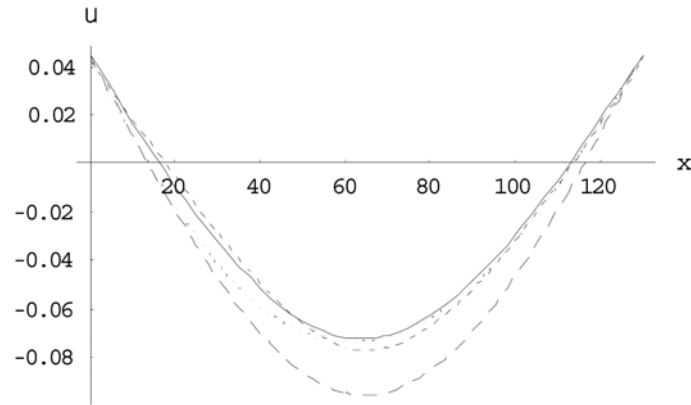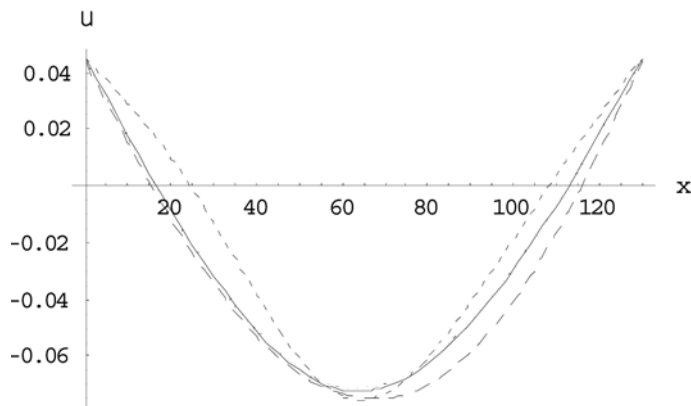
Fig. 14 Displacement of the bridge for $I_{pylon} = 0.2 \text{ m}^4$, and for pier heights $h_1 = 10 \text{ m}$, at $t = 0.518$ (____), $h_1 = 30 \text{ m}$, at $t = 0.458$ (....), $h_1 = 50 \text{ m}$, at $t = 0.613$ (_ _ _), and $h_1 = 70 \text{ m}$, at $t = 0.527$ (__ __)
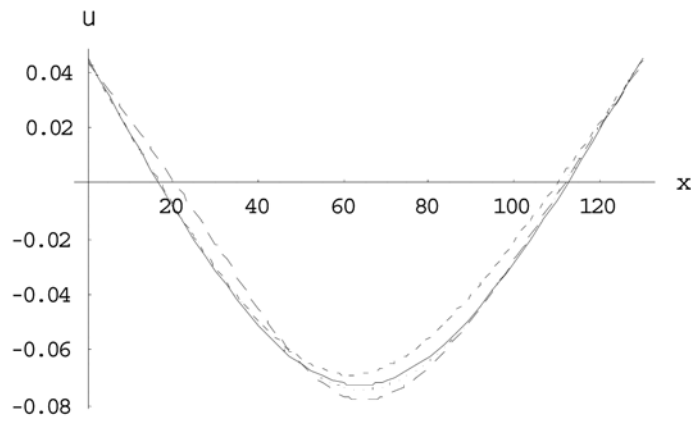
Fig. 15 Displacement of the bridge for $I_{pylon} = 0.8 \text{ m}^4$, and for pier heights $h_1 = 10 \text{ m}$, at $t = 0.484$ (____), $h_1 = 30 \text{ m}$, at $t = 0.495$ (....), $h_1 = 50 \text{ m}$, at $t = 0.430$ (_ _ _), and $h_1 = 70 \text{ m}$, at $t = 0.590$ (__ __)

Fig. 16 Displacement of the bridge for $I_{pylon} = 2 \text{ m}^4$, and for pier heights $h_1 = 10 \text{ m}$, at $t = 0.511$ (____), $h_1 = 30 \text{ m}$, at $t = 0.561$ (....), $h_1 = 50 \text{ m}$, at $t = 0.520$ (_ _ _), and $h_1 = 70 \text{ m}$, at $t = 0.591$ (__ __)

4.3 Effect of the piers' height (three-span bridge)

In this section, we will study, mainly, the effect of the piers' height on the dynamic behavior of the bridge. We will examine, also, the influence of differential movements of the piers, based on mid-quality soil, for an earthquake of distant source. For the present purposes, we consider a three-span bridge with a deck that has the same properties as those of the example given in Section §4.1, and spans of lengths $L_1 = 60$ m, $L_2 = 70$ m, and $L_3 = 60$ m, and middle supports lying on the top of piers with heights h_1, and h_2.

4.3.1 Differential movement of the soil

To study the effect of the piers' height, we assume that the movement of the ground along the length of the bridge is governed by the equation: $f = a \cdot e^{-bt} \sin \omega_e t$, on mid-quality soil, where a, b, ω_e, and k, ρ, have been given in Section 4.1. The eigenfrequencies of the three-span beam can be computed as: $\omega_1 = 34.810$, $\omega_2 = 49.724$, and $\omega_3 = 63.651$ sec^{-1}, and those of the cantilever as:

$$\overline{\omega}_n = \sqrt{\frac{\lambda_n^4 EI_{pylon}}{m_{pylon}}}, \text{ where } \lambda_1 = 1.875/h_1, \lambda_2 = 1.5\,\pi/h_1, \lambda_3 = 2.5\,\pi/h_1, \text{ along with } m_{pylon} = 1000 \text{ kg/m and}$$

$I_{pylon} = 0.20$ m^4, and 2.00 m^4.

Using the influence functions and shape functions and applying the procedure of Section 3, one can solve the integral differential system to obtain the time functions $\varphi_j(t)$, along with the aid of Eq. (1), and study the influence of the height h_1 on the displacement $w(x, t)$ of the bridge deck. Figs. 17, 18, and 19 show the oscillations of the middle supports (as indicated by the functions $\varphi_1(t)$ and $\varphi_2(t)$) for piers with the same height and $I_{pylon} = 0.2$ m^4.

Figs. 20, 21, and 22 show the oscillations of the middle supports (as indicated by the functions $\varphi_1(t)$ and $\varphi_2(t)$) for piers with the same height and $I_{pylon} = 2$ m^4.

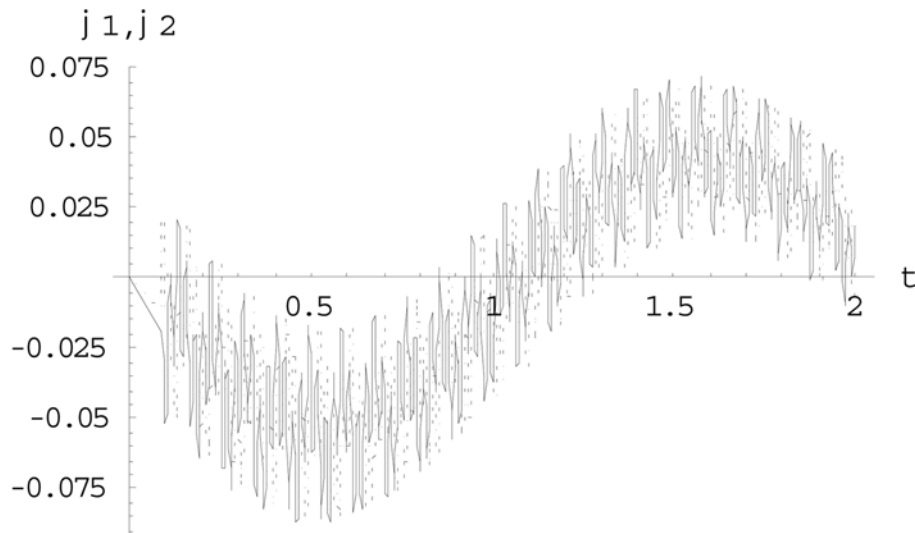Fig. 17 Time functions φ_1 (___) and φ_2 (.....) for $H_1 = H_2 = 20$ m, and $I_{pylon} = 0.2$ m^4
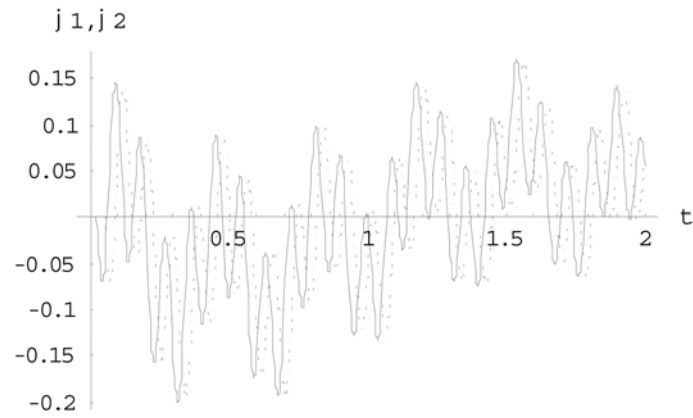
Fig. 18 Time functions φ_1 (___) and φ_2 (.....) for $H_1 = H_2 = 40$ m, and $I_{pylon} = 0.2$ m^4
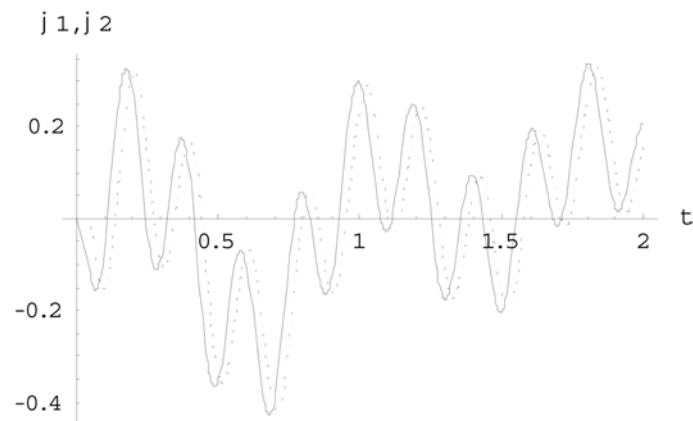

Fig. 19 Time functions φ_1 (___) and φ_2 (.....) for $H_1 = H_2 = 60$ m, and $I_{pylon} = 0.2$ m^4
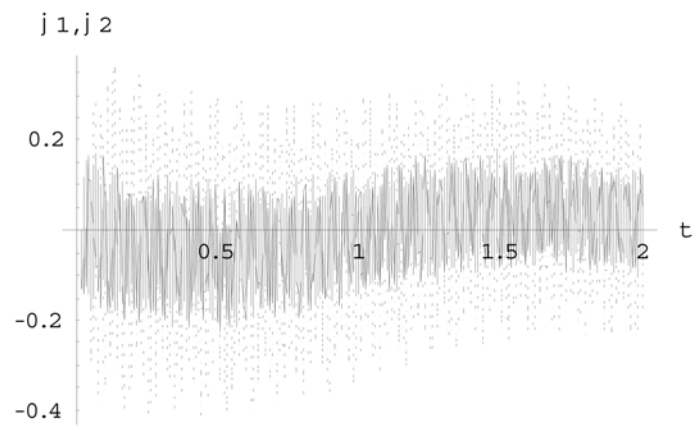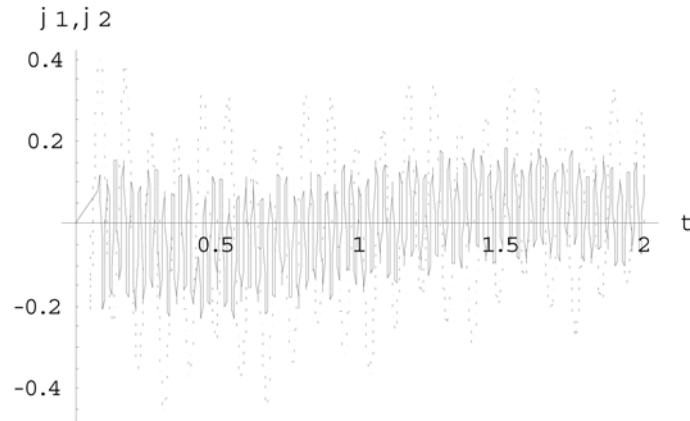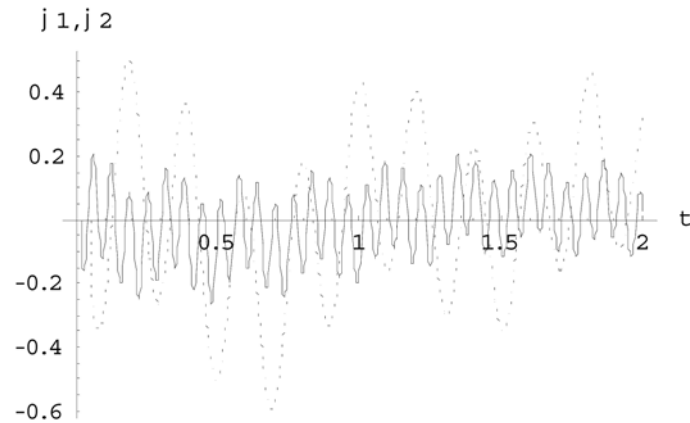

Fig. 20 Time functions φ_1 (___) and φ_2 (.....) for $H_1 = H_2 = 20$ m, and $I_{pylon} = 2$

Fig. 21 Time functions φ_1 (___) and φ_2 (.....) for $H_1 = H_2 = 40$ m, and $I_{pylon} = 2$

Fig. 22 Time functions φ_1 (___) and φ_2 (.....) for $H_1 = H_2 = 60$ m, and $I_{pylon} = 2$

4.3.2 Effect of the piers' height

The effect of the piers' height for $f_0 = f_1 = f_2 = f_3$ can be appreciated from Figs. 23 and 24 for $I_{pylon} = 0.2$ and 2 m^4, respectively, for rather short piers. As can be seen, such an effect is quite significant, even for two piers with a small difference in height.

The effect of the piers' height for $f_0 = f_1 = f_2 = f_3$ can be observed from Figs. 25 and 26 for $I_{pylon} = 0.2$ and 2 m^4, respectively, for taller piers. It appears to be greater than that for short piers, even for the case of two piers with a small difference in height.

Fig. 27 shows the influence of differential movements of the piers caused by the foundation on mid-quality soil. Each curve in this figure has been drawn for the instant when the maximum response occurs.

Fig. 28 shows the displacement of the bridge at different instants for $f_0 = f_1 = f_2 = f_3$, but with equal piers' height. In contrast, Fig. 29 shows the displacement of the bridge at different instants, but for piers located at mid-quality soil. Finally, Fig. 30 shows the displacement of the bridge at different instants for $f_0 = f_1 = f_2 = f_3$, and piers with different heights.
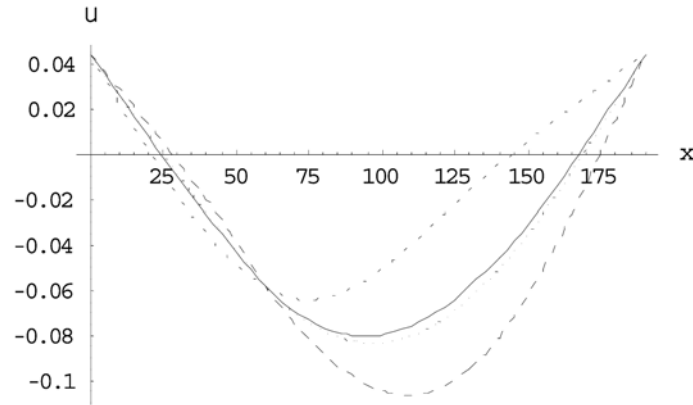
Fig. 23 Displacement of the bridge for $I_{pylon} = 0.2$ m^4, $f_o = f_1 = f_2 = f_3$, and for pier heights $h_1 = 20$ m, and $h_2 = 20$ m (____), $h_2 = 22$ m (….), $h_2 = 24$ m (_ _ _), $h_2 = 26$ m (__ __)
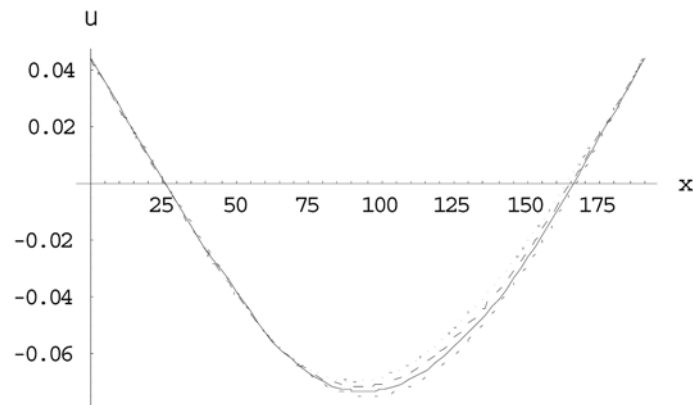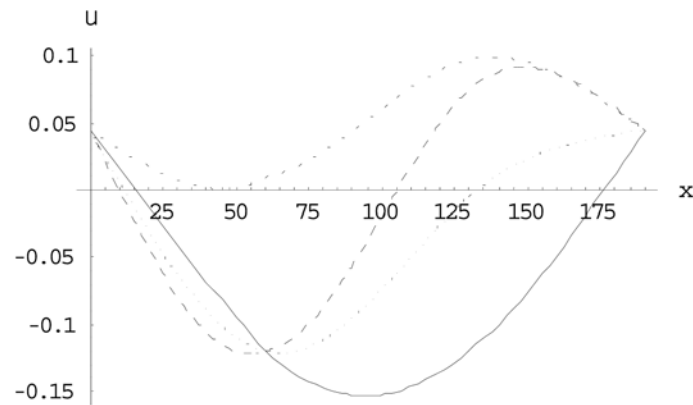

Fig. 24 Displacement of the bridge for $I_{pylon} = 2$ m^4, $f_o = f_1 = f_2 = f_3$, and for pier heights $h_1 = 20$ m, and $h_2 = 20$ m (____), $h_2 = 22$ m (….), $h_2 = 24$ m (_ _ _), $h_2 = 26$ m (__ __)

Fig. 25 Displacement of the bridge for $I_{pylon} = 0.2$ m^4, $f_o = f_1 = f_2 = $ f$_3$, and for pier heights $h_1 = 40$ m, and $h_2 = 40$ m (____), $h_2 = 42$ m (….), $h_2 = 44$ m (_ _ _), $h_2 = 46$ m (__ __)
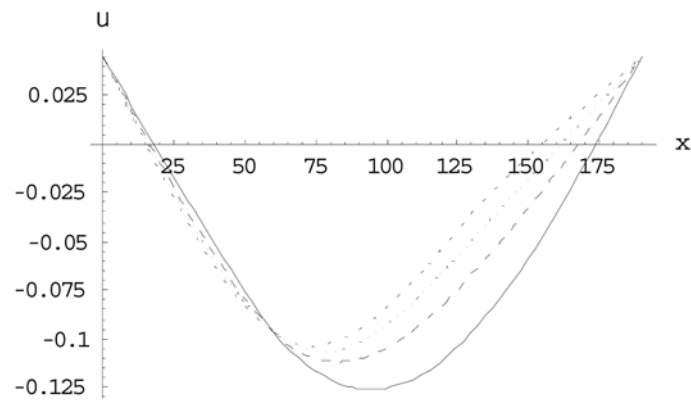
Fig. 26 Displacement of the bridge for $I_{pylon} = 2$ m^4, $f_o = f_1 = f_2 = f_3$, and for pier heights $h_1 = 40$ m, and $h_2 = 40$ m (_____), $h_2 = 42$ m (….), $h_2 = 44$ m (_ _ _), $h_2 = 46$ m (__ __)
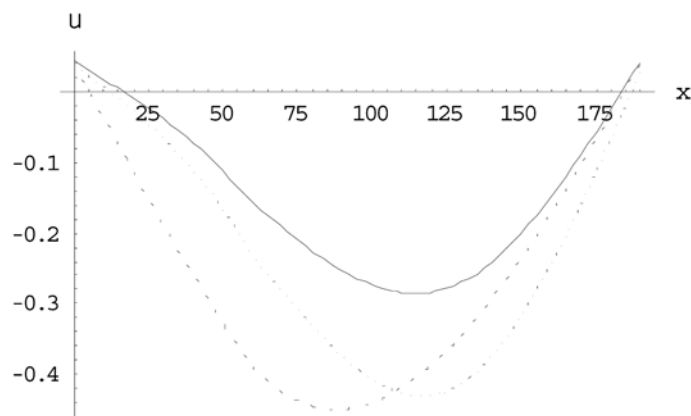

Fig. 27 Displacement of the bridge for $I_{pylon} = 0.2$ m^4, based on mid-soil, and for pier heights: $h_1 = h_2 = 20$ m, at $t = 0.55$ sec, (_____), $h_1 = h_2 = 40$ m, at $t = 0.32$ sec (….), and $h_1 = h_2 = 60$ m, at $t = 0.65$ sec (_ _ _)

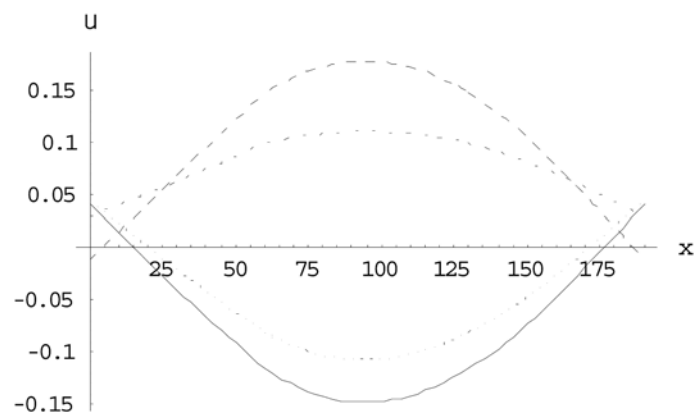
Fig. 28 Displacement of the bridge for $I_{pylon} = 0.2$ m^4, $f_o = f_1 = f_2 = f_3$, $h_1 = h_2 = 40$ m, at $t = 0.38$ sec, (_____), $t = 0.47$ sec (….), $t = 0.79$ sec (_ _ _), and $t = 1.15$ sec (__ __)
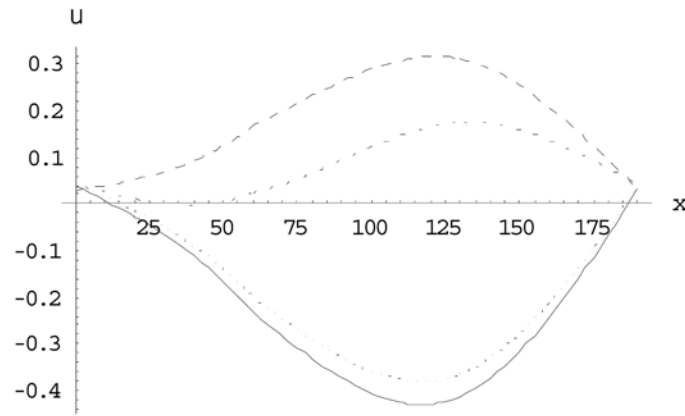
Fig. 29 Displacement of the bridge for I_{pylon} = 0.2 m^4, based on mid-soil, $h_1 = h_2$= 40 m, at t = 0.32 sec, (____), t = 0.40 sec (….), t = 0.63 sec (_ _ _), and t = 0.81 sec (__ __)
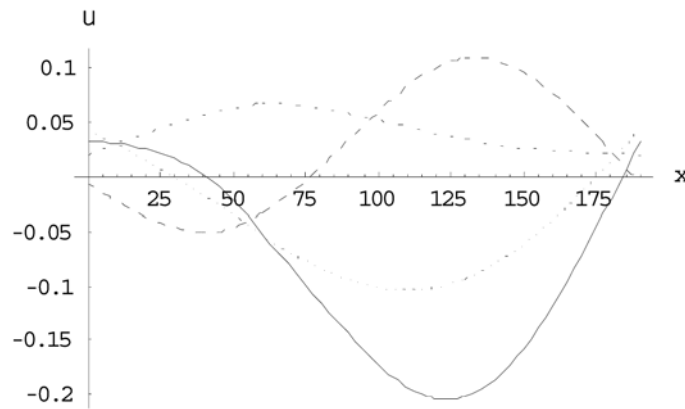

Fig. 30 Displacement of the bridge for I_{pylon} = 0.2 m^4, $f_o = f_1 = f_2 = f_3$, h_1 = 40 m, h_2 = 45 m, at t = 0.26 sec, (____), t = 0.60 sec (….), t = 0.88 sec (_ _ _), and t = 1.10 sec (__ __)

5. Conclusions

In this work, a simple mathematical model is proposed of multi-span steel bridges resting on pylons with different heights, based on which the dynamic response of the bridges is studied. From the analyses and numerical examples presented herein, the following conclusions can be drawn:

a. For the cases studied in Section 4, the maximum displacement amplitude occurs during the first cycles of oscillation of the bridge (for $h/L < 0.20$), while this same maximum may appear during the second or the third cycle (for $h/L > 0.20$)

b. Different ground qualities will result in different movements at the supports, thereby affecting the displacement of the bridge. This effect, for the model studied, ranges from 0% to 3% for a granite soil, and from 3.5% to 28% for a mud soil, where the smaller limits correspond to low frequency motions and the higher limits correspond to high frequency motions.

c. We understand that pure mud soil may not be realistic in practice. Thus, such a significant

reduction of the motion, as exhibited in the figures of Section 4 associated with mud soil, may not be realistic for piers with such small distances from 60 to 190 m, as those of the examples studied. It is also clear though, that one must take into account a possible notable reduction of the ground motion for soils with poor qualities.

 d. The properties of the piers (i.e. height and rigidity) affect strongly the oscillations of the bridge.

 e. An increase in the height of the piers, for the models studied, can cause a 50% increase in the displacement of the bridge for $I_{pylon} = 0.2$, while for $I_{pylon} = 2.0$ the increase in displacement drops to 4%.

 f. The numerical examples have indicated that depending on the design of the piers, one can achieve a satisfactory decrease of the maximum displacements and thus, a better dynamic behavior of the bridge.

 g. From Figs. 23 to 30, one observes that the transversal dynamic distress and the distribution of bending moments (caused by earthquakes) should be studied with great caution, since there may occur situations that are significantly different from those under static loadings as implied by a design.

References

Abrahamson, N.A., Schneider, J.F. and Stepp, J.C. (1991), "Empirical spatial coherency functions for application to soil-structures interaction analyses", *Earthq. Spectra,* **7**(1), 41-54.

Betti, R., Abdel-Ghaffar, A.M. and Niazy, A.S. (1993), "Kinematic soil-structure interaction for long-span cable-supported bridges", *Earthq. Eng. Struct. D.*, **22**(5), 415-430.

Bogdanoff, J.L., Goldberg, J.E. and Schiff, A.J. (1965), "The effect of ground transmission time on the response of long structures", *B. Seismol. Soc. Am.*, **55**, 627-640.

ENV 1998-2, *Eurocode 8-Part 2 (EC8-2) : Bridges*, (2002), European Committee for Standardization, Brussels.

Harichandran, R.S. and Wang, W. (1990), "Response of indeterminate two-span beam to spatially varying seismic excitation", *Earthq. Eng. Struct. D.*, **19**, 173-187.

Michaltsos, G.T. (2005), *Dynamic problems of Steel Bridges*, Ed. Symeon, Athens, (in Greek).

Monti, G., Nuti, C. and Pinto, P. (1996), "Nonlinear response of bridges under multisupport excitation", *J. Struct. Eng-ASCE,* **122**(10), 1147-1158.

Nikolaou, A., Mylonakis, G., Gazetas, G. and Tazoh, T. (2001), "Kinematic pile bending during earthquakes: Analysis and measurements", *Geotechnique,* **51**(5), 425-440.

Price, T.E. and Eberhard, M.O. (1998), "Effects of spatially varying ground motions on short bridges", *J. Struct. Eng-ASCE,* **124**(8), 948-955.

Wylie, C.R. (1975), *Advanced Engineering Mathematics,* McGraw-Hill Kogakusha, Ltd., Tokyo.

Zerva, A. (1990), "Response of multi-span beams to spatially incoherent seismic ground motions", *Earthq. Eng. Struct. D.*, **19**(6), 819-832.

Zerva, A. (1999), "Spatial variability of seismic motions recorded over extended ground surface areas", *Wave motion in earthquake engineering,* Eds., E. Kausel & G. Manolis, MIT Press, Cambridge, Mass.

Appendix

Influence functions (Michaltsos 2005)

One-span beam
 Subside of the support number 0: $g(x) = 1 - x/l$
 Subside of the support number 1: $g(x) = x/l$
Fixed-joined beam
 Subside of the fixed end: $g(x) = 1$

 Subside of the free end: $g(x) = \dfrac{3x^2}{2l^2} - \dfrac{x^2}{2l^3}$

Two-span beam
Subside of the support number 0

$$g_1(x_1) = \frac{(l_1 - x_1)}{l_1} - \frac{1}{2l_1(l_1 + l_2)}\left(-\frac{x_1^3}{l_1} + l_1 x_1\right)$$

$$g_2(x_2) = -\frac{1}{2l_1(l_1 + l_2)}\left(\frac{x_2^3}{l_2} - 3x_2^2 + 2l_2 x_2\right)$$

 Subside of the support number 1

$$g_1(x_1) = \frac{x_1}{l_1} + \frac{1}{2l_1 l_2}\left(-\frac{x_1^3}{l_1} + l_1 x_1\right)$$

$$g_2(x_2) = \frac{l_2 - x_2}{l_2} + \frac{1}{2l_1 l_2}\left(\frac{x_2^3}{l_2} - 3x_2^2 + 2l_2 x_2\right)$$

Subside of the support number 2

$$g_1(x_1) = -\frac{1}{2l_2(l_1 + l_2)}\left(-\frac{x_1^3}{l_1} + l_1 x_1\right)$$

$$g_2(x_2) = \frac{x_2}{l_2} - \frac{1}{2l_2(l_1 + l_2)}\left(\frac{x_2^3}{l_2} - 3x_2^2 + 2l_2 x_2\right)$$

Three-span beam
 Subside of the support number 0

$$g_1(x_1) = \frac{l_1 - x_1}{l_1} - 2\kappa_o(l_1 + l_2)\left(-\frac{x_1^3}{l_1} + l_1 x_1\right)$$

$$g_2(x_2) = -2\kappa_o(l_1 + l_2)\left(\frac{x_2^3}{l_2} - 3x_2^2 + 2l_2 x_2\right) - \kappa_o l_2\left(\frac{x_2^3}{l_2} - l_2 x_2\right)$$

$$g_3(x_3) = \kappa_o l_2\left(\frac{x_3^3}{l_3} - 3x_3^2 + 2l_3 x_3\right)$$

$$\text{where: } \kappa_o = \frac{1}{l_1(3l_2^2 + 4l_1l_2 + 4l_1l_3 + 4l_2l_3)}$$

Subside of the support number 1

$$g_1(x_1) = \frac{x_1}{l_1} + \kappa_1[2l_2(l_2 + l_3) + l_1(2l_2 + 2l_3)]\left(-\frac{x_1^3}{l_1} + l_1x_1\right)$$

$$g_2(x_2) = \frac{l_2 - x_2}{l_2} + \kappa_1[2l_2(l_2 + l_3) + l_1(2l_2 + 2l_3)]\left(\frac{x_2^3}{l_2} - 3x_2^2 + 2l_2x_2\right)$$

$$-\kappa_1(l_1 + l_2)(2l_1 + l_2)\left(-\frac{x_2^3}{l_2} + l_2x_2\right)$$

$$g_3(x_3) = -\kappa_1(l_1 + l_2)(2l_1 + l_2)\left(\frac{x_3^3}{l_3} - 3x_3^2 + 2l_3x_3\right)$$

$$\text{where: } \kappa_1 = \frac{1}{l_1l_2(3l_2^2 + 4l_1l_2 + 4l_1l_3 + 4l_2l_3)}$$

Subside of the support number 2

$$g_1(x_1) = \kappa_2[2l_1(l_2 + l_3) + l_2(2l_2 + 3l_3)]\left(-\frac{x_1^3}{l_1} + l_1x_1\right)$$

$$g_2(x_2) = -\frac{x_2}{l_2} + \kappa_2(l_2 + l_3)(l_2 + 2l_3)\left(\frac{x_2^3}{l_2} - 3x_2^2 + 2l_2x_2\right)$$

$$-\kappa_2[2l_1(l_2 + l_3) + l_2(2l_2 + 3l_3)]\left(-\frac{x_2^3}{l_2} + l_2x_2\right)$$

$$g_3(x_3) = -\frac{l_3 - x_3}{l_3} + \kappa_2[2l_1(l_2 + l_3) + l_2(2l_2 + 3l_3)]\left(\frac{x_3^3}{l_3} - 3x_3^2 + 2l_3x_3\right)$$

$$\text{whrer: } \kappa_2 = \frac{1}{l_2l_3(3l_2^2 + 4l_1l_2 + 4l_1l_3 + 4l_2l_3)}$$

Subside of the support number 3

$$g_1(x_1) = \kappa_3l_2\left(-\frac{x_1^3}{l_1} + l_1x_1\right)$$

$$g_2(x_2) = -l_2\kappa_3\left(\frac{x_2^3}{l_2} - 3x_2^2 + 2l_2x_2\right) - 2\kappa_3(l_1 + l_2)\left(-\frac{x_2^3}{l_2} + l_2x_2\right)$$

$$g_3(x_3) = \frac{x_3}{l_3} - 2\kappa_3(l_1 + l_2)\left(\frac{x_3^3}{l_3} - 3x_3^2 + 2l_3x_3\right)$$

$$\text{whrer: } \kappa_3 = \frac{1}{l_3(3l_2^2 + 4l_1l_2 + 4l_1l_3 + 4l_2l_3)}$$

Borel's theorem (or the theorem of convolution)

If $Lf_1(t) = g_1(p)$ and $Lf_2(t) = g_2(p)$, then the following relation is valid

$$L\int_0^t f_1(\tau)f_2(t-\tau)d\tau = g_1(p)g_2(p)$$